Available online at www.sciencedirect.com
ScienceDirect
Bioorganic & Medicinal Chemistry Letters 17 (2007) 5390–5395
Bioorganic & Medicinal Chemistry Letters

Kinesin spindle protein (KSP) inhibitors. Part 6: Design and synthesis of 3,5-diaryl-4,5-dihydropyrazole amides as potent inhibitors of the mitotic kinesin KSP

Paul J. Coleman,[a,*] John D. Schreier,[a] Christopher D. Cox,[a] Mark E. Fraley,[a] Robert M. Garbaccio,[a] Carolyn A. Buser,[b] Eileen S. Walsh,[b] Kelly Hamilton,[b] Robert B. Lobell,[b] Keith Rickert,[b] Weikang Tao,[b] Ronald E. Diehl,[b] Vicki J. South,[b] Joseph P. Davide,[b] Nancy E. Kohl,[b] Youwei Yan,[c] Lawrence Kuo,[c] Thomayant Prueksaritanont,[d] Chunze Li,[d] Elizabeth A. Mahan,[d] Carmen Fernandez-Metzler,[d] Joseph J. Salata[e] and George D. Hartman[a]

[a]*Department of Medicinal Chemistry, Merck Research Laboratories, PO Box 4, Sumneytown Pike, West Point, PA 19486, USA*
[b]*Department of Cancer Research, Merck Research Laboratories, PO Box 4, Sumneytown Pike, West Point, PA 19486, USA*
[c]*Department of Structural Biology, Merck Research Laboratories, PO Box 4, Sumneytown Pike, West Point, PA 19486, USA*
[d]*Department of Drug Metabolism, Merck Research Laboratories, PO Box 4, Sumneytown Pike, West Point, PA 19486, USA*
[e]*Department of Cellular Safety, Merck Research Laboratories, PO Box 4, Sumneytown Pike, West Point, PA 19486, USA*

Received 1 June 2007; revised 27 July 2007; accepted 30 July 2007
Available online 6 August 2007

Abstract—3,5-Diaryl-4,5-dihydropyrazoles were discovered to be potent KSP inhibitors with excellent in vivo potency. These enzyme inhibitors possess desirable physical properties that can be readily modified by incorporation of a weakly basic amine. Careful adjustment of amine basicity was essential for preserving cellular potency in a multidrug resistant cell line while maintaining good aqueous solubility.

Small molecule inhibitors of kinesin spindle protein are anti-mitotic agents that have clinical potential for the treatment of cancer.[1] Unlike anti-mitotic treatments that directly target tubulin (e.g., taxanes, vinca alkaloids), KSP inhibitors act upon a motor protein (KSP or *Hs* Eg5) that drives the separation of centrosomes during mitosis.[2] Inhibition of KSP halts mitosis affording a characteristic monoastral phenotype which eventually leads to cell death in transformed cells.[3] Compared with current tubulin-targeting agents, KSP inhibitors may offer distinct advantages in having a novel resistance profile and a reduced potential for neurotoxicity. Several KSP inhibitors are currently in clinical trials to evaluate this mechanism as a potential cancer therapy.[4]

Previous publications from this laboratory have described efforts to design and synthesize small molecule KSP inhibitors based on diaryl dihydropyrazole and dihydropyrrole scaffolds.[5] Preferred aryl substitutions in these two series have been established with considerable overlap in structure–activity relationships between the two. We have recently reported an important advance in the design of these enzyme inhibitors where incorporation of a weakly basic amine tethered to the 2-position of the dihydropyrrole core conferred aqueous solubility, enhanced enzyme inhibitory potency, and maintained cellular activity in a P-glycoprotein (Pgp) over-expressing cell line.

An important design consideration for our leading KSP inhibitors is to maintain cellular potency in

Keywords: Cancer; Kinesin spindle protein; KSP inhibitors; Antimitotics; Dihydropyrazoles; P-Glycoprotein.
* Corresponding author. Tel.: +1 215 652 4618; fax: +1 215 652 7310; e-mail: paul_coleman@merck.com

0960-894X/$ - see front matter © 2007 Elsevier Ltd. All rights reserved.
doi:10.1016/j.bmcl.2007.07.046

chemoresistant cell lines including cell lines that overexpress Pgp. Pgp is an ATP-dependent efflux pump that recognizes a broad set of substrates and reduces cellular concentrations of chemotherapeutic agents. This efflux transporter is upregulated by the human MDR1 gene. Overexpression confers a multi-drug resistance phenotype to cells and may play a role in clinical resistance to known anti-mitotic agents.[6]

In a recent publication, we disclosed that Pgp transport correlated with amine basicity for dihydropyrrole inhibitors.[5e] Indeed, incorporation of β,β-difluorosubstitution to provide compound **1** moderates basicity, preserves aqueous solubility, and maintains potency in a multidrug resistant cell line (MDR+). However difluorination of **1** is associated with a general increase in lipophilicity and modest in vivo activity. In this paper, we describe how dihydropyrazole amides were modified by appending weakly basic amines in analogy to the efforts we have reported in the dihydropyrrole urea series. These pyrazole amides have distinct advantages with an overall reduced propensity for Pgp efflux, enhanced physical properties, and an improved in vivo profile.

Our efforts reported in this manuscript are focused on dihydropyrazole amides (e.g., **12**) as KSP inhibitors (Table 1). A straightforward synthesis of dihydropyrazole amides is shown in Scheme 1.[7] Commercially available 3-pentyn-1-ol **2** was protected as a tetrahydropyranyl ether. Lithiation of the alkynyl ether with *n*-butyllithium followed by acylation with Weinreb amide **3** provided adduct **4** in excellent yield. Diphenyl cuprate addition to **4** provided adduct **5** as a mixture of olefin isomers in good yield. Treatment of **5** with hydrazine hydrate in pyridine with microwave heating followed by cooling to 0 °C and treatment with acetyl chloride provided the acetylated dihydropyrazole **6**. Acidic deprotection of **6** with TsOH afforded primary alcohol **7** in good overall yield. Racemic alcohol **7** could be resolved by chiral HPLC to provide the desired 5*S*-enantiomer.[8] Oxidation of the primary alcohol with Dess–Martin periodinane gave an aldehyde that was transformed by reductive alkylation to provide the KSP inhibitors **11**–**21**.

As shown in Table 1, pyrazole urea **10** is equipotent[9] to pyrrole urea **9** with an improved MDR ratio. The MDR ratio is calculated by comparing the cellular potency (G2/M arrest) of a KSP inhibitor in a wild-type KB-3-1 human epidermoid carcinoma cell line versus the cellular potency in a Pgp-over-expressing KB cell line.[10] The ratio of these numbers ($Pgp^{+}EC_{50}$/wt EC_{50}) is reported as the MDR ratio. In this assay, Taxol has an MDR ratio of ca. 25×10^3. In our view, a compound with an MDR ratio <10 is desirable, and a value of 1 is ideal. Replacing the dimethyl urea with an acetyl group in **11** maintains potency and further reduces the MDR ratio. Presumably, as a hydrogen-bond acceptor, the urea in **10** is a contributor to Pgp susceptibility. A further improvement in the

Table 1. Dihydropyrazole Inhibitors: Amides vs. Ureas

	Compound	KSP IC_{50}[a] (nM)	MDR ratio[a]
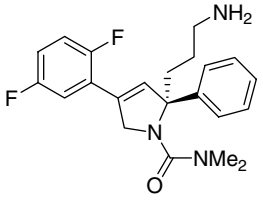	**9**	2.2	1204
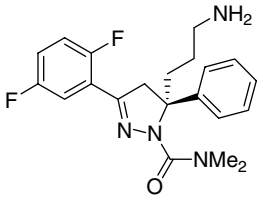	**10**	2.0	491
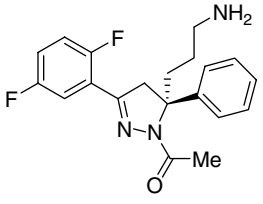	**11**	0.9	88
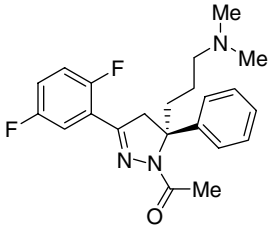	**12**	1.4	4.4

All values are reported for $n = 3$ or greater with standard deviations within 25–50% of the reported value.
[a] See Refs. 9 and 10 for assay details.

MDR ratio is attained when the primary amine in **11** is replaced with a tertiary amine as in **12**.[11]

Based on these data, we refocused our efforts on compounds related to **12** where various tertiary amines were introduced onto the C-5 side chain. Potency for these analogs is shown in Table 2. Enzyme potency was maintained across a diverse set of substituted tertiary amines.

The crystal structures of the binary KSP-ADP and ternary KSP-ADP-inhibitor complexes have been solved for multiple compounds in the dihydropyrazole series, including compound **14**. These structures reveal a unique loop, denoted L5, that is flexible and solvent-exposed in the binary structure. The L5-loop folds down to trap the inhibitor in a surface pocket in the ternary structure. This novel binding site is distinct from the ATP and microtubule binding sites and gives rise to allosteric enzyme inhibition.[12] Tethered tertiary amines such as the morpholine in **14** are exposed to solvent in the solid state. Consistent with

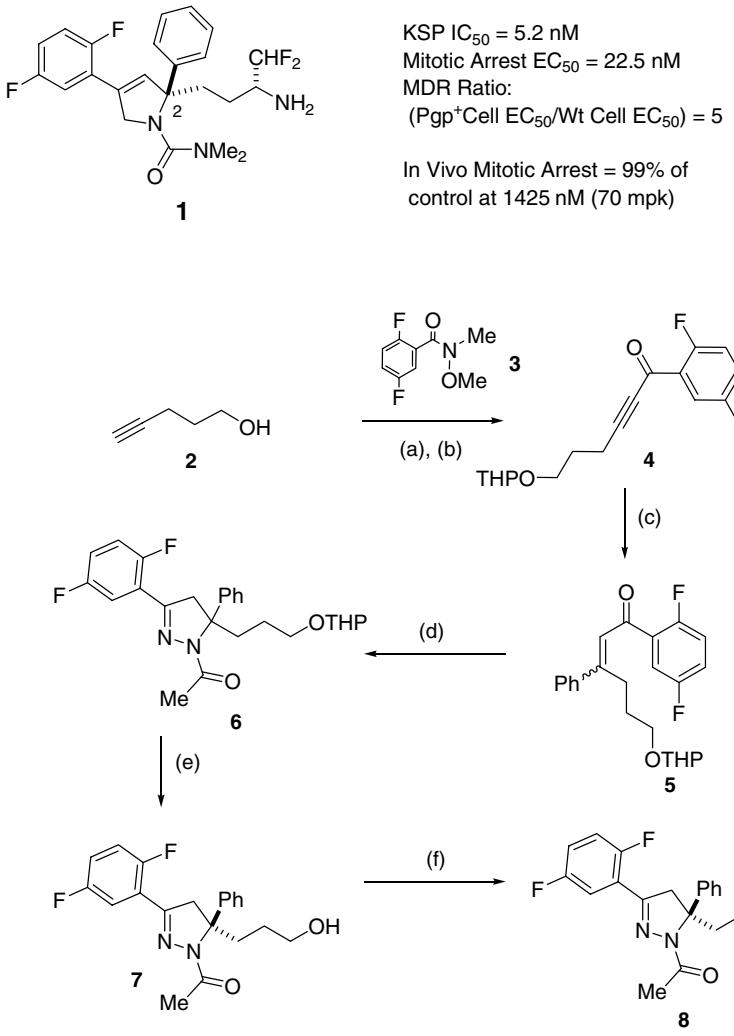

Scheme 1. General synthesis of 1,4-diaryl-4,5-dihydropyrazole KSP inhibitors. Reagents and conditions: (a) DHP, TsOH; (b) *n*-BuLi, then **3**, THF −78 °C, 92%; (c) PhLi, CuBr–DMS, THF, 95%; (d) H_2 NNH_2–H_2O, pyridine, 90 °C, 30 min then cool to 0 °C, AcCl; (e) TsOH, MeOH, then chiral HPLC 79% for three steps; (f) Dess–Martin periodinane, DCM, 80% R_1R_2NH; $NaBH(OAc)_3$.

this mode of binding is the fact that increasing the steric bulk of the tertiary amine had no significant impact on enzyme potency. Cellular potency was maintained in most instances. Interestingly, single fluorine substitution was tolerated in **19**; however, installation of a second fluorine atom in **20** decreased cell potency, presumably due to reduced cell permeability as a result of greater lipophilicity.

As previously noted in a related series of pyrrole-based KSP inhibitors,[5e] the MDR ratio correlated closely with amine basicity (Table 3) for compounds in this class. Lowering the pK_a (below ~8) of the tertiary amine causes a significant attenuation in the MDR ratio. Interestingly, these pyrazole amides had a greater tolerance for basicity than the corresponding pyrrole ureas. KSP inhibitor **13** possessed excellent intrinsic and cellular potencies and a low Pgp susceptibility (MDR ratio = 2.5). This compound was chosen for in vivo evaluation in a pharmacodynamic model of G2/M arrest.

Aqueous solutions of compound **13** of increasing doses were administered to nude mice bearing A2780 xenograft implants via Alzet osmotic pumps.[13] The mice were then sacrificed after 22 h and the tumors were removed and sectioned. The sections were stained for phospho-histone H3, an inducible marker of mitotic arrest. Minimal plasma concentrations associated with maximal mitotic arrest in the tumor were determined. In this model KSP inhibitor **13** induced maximal mitotic arrest with a plasma exposure of 56 nM. The concentration of compound **13** was not measured in the tumor. Compound **13** has similar protein binding in both mice (92%) and human (91%) plasma suggesting that compound **13** could provide a similar level of pharmacodynamic potency in human. This level of in vivo potency represents a >20-fold improvement over pyrrole urea **1**.[14]

A potential limiting feature of **13** and several structurally related tertiary amines from this series was a propensity to induce QTc prolongation in a canine cardiovascular model at low micromolar (<10 μM) exposures.[15] The ECG changes associated with **13** were not predicted by hERG binding (IC_{50} > 30,000 nM); however blockade of the IKr current by **13** could be

Table 2. Side-chain amine SAR

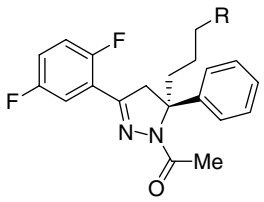

Compound	R	KSP IC_{50} (nM)	Cell potency[a] (nM)
11		0.9	2.6
12		1.4	2.3
13	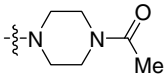	2.8	6.0
14	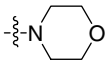	1.8	11
15	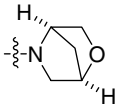	1.0	2.8
16[b]	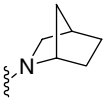	1.0	2.4
17	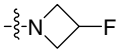	1.8	7.2
18		1.3	3.1
19	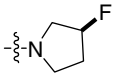	1.0	1.8
20	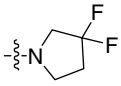	4.0	55
21	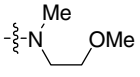	2.0	7.0

[a] EC_{50} for G2/M block in A2780 cell line.
[b] Approximately 1:1 mixture of diastereomers.

measured in a classical patch clamp assay.[16] This activity reduced the potential safety margins associated with **13**. Fortunately, the primary amine **11** was not a potent functional inhibitor of IKr and efforts were refocused on compounds related to **11** that lacked a tertiary amine.

Table 3. Mitotic arrest MDR ratio as a function pK_a

Compound	pK_a[a]	Mitotic arrest MDR ratio
16	10.1	31
18	9.4	10
15	8.0	3.4
14	7.1	1.7
17	7.1	1.1
13	6.7	2.5

[a] Values were determined with a Sirius GLp$K_a$titrator, average of $n = 3$ determinations.

In order to attenuate the Pgp efflux issues associated with primary amine **11**, single β-fluorine substitution was probed proximal to the appended amine. Both the (5*S*,2′*S*) and (5*S*,2′*R*) β-fluoroamine diastereomers were studied in detail. Preparation of the (5*S*,2′*S*) diastereomer is shown in Scheme 2. Primary alcohol **7** was efficiently oxidized to the carboxylic acid with chromium trioxide and transformed to acyl oxazolidinone **22**. Diastereoselective fluorination of the sodium enolate of **23** with $(PhO_2S)_2NF$ gave compound **23** with greater than 20:1 selectivity for the 2′*S*-fluoro substitution.[17] Notably, racemic substituted pyrazole **7** could be carried through this route and the diastereomers associated with compound **23** could be separated on silica gel. Transformation of **23** to amine **24** was straightforward.

Although both diastereomers were potent KSP inhibitors,[18] the 5*S*,2′*S* diastereomer **24** had superior pharmacokinetic properties (dog $T_{1/2} = 9$ h vs 4.3 h) and was the subject of additional study. Compound **24** had reduced potential for IKr blockade based on its potency in a functional patch clamp assay ($EC_{50} > 30$ μM). Indeed when evaluated in the same cardiovascular dog model as compound **13**, KSP inhibitor **24** showed no propensity for ECG interval changes with exposures as great as 40 μM. When evaluated in the mouse xenograft at 3 mpk, compound **24** provided a full mitotic arrest with circulating plasma levels of 38 nM. As predicted from our previous observations, potency for compound **24** was maintained in a Pgp over-expressing KB cell line (MDR ratio = 5). Summary data for compound **24** relative to compound **1** are shown in Table 4.

We have demonstrated that pyrazole amides such as **24** are potent KSP inhibitors that have a lower intrinsic susceptibility for Pgp efflux relative to pyrrole ureas such as **1** with a greater tolerance of basicity on the appended side chain. Because of this, single β-fluorine substitution preserves cellular potency in Pgp over-expressing cells without compromising physical properties and in vivo activity. Additionally, KSP inhibitor **24** has highly favorable pharmacokinetics with a plasma half-life of 9 h in dogs. Unlike appended tertiary amines in this series, compound **24** does not cause QTc changes in the

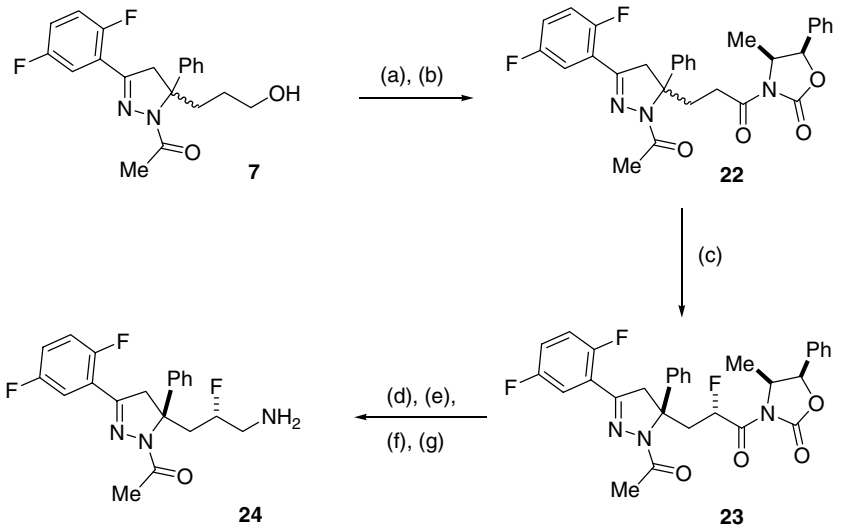

Scheme 2. Reagents: (a) H_5IO_6/CrO_3, H_2O/MeCN, 99%; (b) $SOCl_2$ then (4*R*,5*S*)-4-methyl-5-phenyl-2-oxazolidinone/*n*-BuLi, 79%; (c) NaHMDS, $(PhO_2S)_2NF$, 39% (50% theoretical); (d) $LiBH_4$; (e) MsCl, Et_3N; (f) NaN_3, DMF, 47% (three steps); (g) Pd/C, H_2, 90%.

Table 4. Comparative data for compounds **1** and **24**

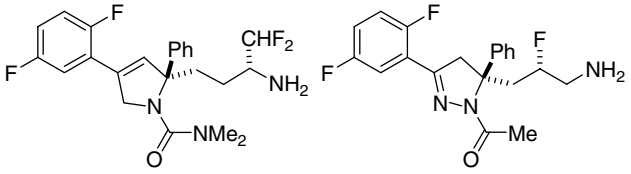

	1	**24**
KSP IC_{50}	5.2 nM	0.82 nM
Mitotic arrest (EC_{50})	22.5 nM	3.4 nM
In vivo mitotic arrest (EC_{50})	1425 nM	38 nM
MDR ratio	5.2	5.2
Dog PK (iv, 0.25 mpk)	$T_{1/2}$ = 3.2 h V_{dss} = 2.8 L/kg Cl = 16.5 mL/min/kg	$T_{1/2}$ = 9.0 h V_{dss} = 6.3 L/kg Cl = 11.1 mL/min/kg

dog. Additional studies on related dihydropyrazole-based KSP inhibitors will be described in the following two papers.

Acknowledgments

The authors thank Dr. Chuck Ross, Dr. Harri Ramjit, and Joan Murphy for high resolution mass spectral analyses. We thank Matt Zrada for determining pK_a values. We also acknowledge Lazlo Kiss for high-throughput electrophysiology studies.

References and notes

1. Miglarese, Mark R.; Carlson, Robert O. *Expert Opin. Investig. Drugs* **2006**, *15*, 1411.
2. Mayer, T. U.; Kapoor, T. M.; Haggarty, S. J.; King, R. W.; Schreiber, S. L.; Mitchison, T. J. *Science* **1999**, *286*, 971.
3. Tao, Weikang; South, Victoria J.; Diehl, Ronald E.; Davide, Joseph P.; Sepp-Lorenzino, Laura; Fraley, Mark E.; Arrington, Kenneth L.; Lobell, Robert B. *Mol. Cell. Biol.* **2007**, *27*, 689.
4. (a) Jackson, J. R.; Patrick, D. R.; Dar, M. M.; Huang, P. S. *Nat. Rev. Cancer* **2007**, *7*, 107; (b) Sorbera, L. A.; Bolós, N.; Serradell, N.; Bayés, M. *Drugs Future* **2006**, *31*, 778; (c) Duhl, David M.; Renhowe, Paul A. *Curr. Opin. Drug Discov. Devel.* **2005**, *8*, 431.
5. (a) Cox, C. D.; Breslin, M. J.; Mariano, B. J.; Coleman, P. J.; Buser, C. A.; Walsh, E. S.; Hamilton, K.; Huber, H. E.; Kohl, N. E.; Torrent, M.; Yan, Y.; Kuo, L. C.; Hartman, G. D. *Bioorg. Med. Chem. Lett.* **2005**, *15*, 2041; (b) Fraley, M. E.; Garbaccio, R. M.; Arrington, K. L.; Hoffman, W. F.; Tasber, E. S.; Coleman, P. J.; Buser, C. A.; Walsh, E. S.; Hamilton, K.; Schaber, M. D.; Lobell, R. B.; Tao, W.; South, V. J.; Yan, Y.; Kuo, L. C.; Prueksaritanont, T.; Shu, C.; Torrent, M.; Heimbrook, D. C.; Kohl, N. E.; Huber, H. E.; Hartman, G. D. *Bioorg. Med. Chem. Lett.* **2006**, *16*, 1775; (c) Garbaccio, R. M.; Fraley, M. E.; Tasber, E. S.; Olson, C. M.; Hoffman, W. F.; Torrent, M.; Buser, C. A.; Walsh, E. S.; Hamilton, K.; Schaber, M. D.; Lobell, R. B.; Tao, W.; South, V. J.; Yan, Y.; Kuo, L. C.; Prueksaritanont, T.; Slaughter, D. E.; Shu, C.; Heimbrook, D. C.; Kohl, N. E.; Huber, H. E.; Hartman, G. D. *Bioorg. Med. Chem. Lett.* **2006**, *16*, 1780; (d) Cox, C. D.; Torrent, M.; Breslin, M. J.; Mariano, B. J.; Whitman, D.

B.; Coleman, P. J.; Buser, C. A.; Walsh, E. S.; Hamilton, K.; Schaber, M. D.; Lobell, R. B.; Tao, W.; South, V. J.; Kohl, N. E.; Yan, Y.; Kuo, L. C.; Prueksaritanont, T.; Slaughter, D. E.; Li, C.; Mahan, E.; Lu, B.; Hartman, G. D. *Bioorg. Med. Chem. Lett.* **2006**, *16*, 3175; (e) Cox, C. D.; Breslin, M. J.; Coleman, P. J.; Garbaccio, R. M.; Fraley, M. E.; Zrada, M. M.; Buser, C. A.; Walsh, E. S.; Hamilton, K.; Lobell, R. B.; Tao, W.; Abrams, M. T.; South, V. J.; Huber, H. H.; Kohl, N. E.; Hartman, G. D. *Bioorg. Med. Chem. Lett.* **2007**, *17*, 2697.

6. Szakacs, G.; Paterson, J. K.; Ludwig, J. A.; Booth-Genthe, C.; Gottesman, M. M. *Nat. Rev. Drug Disc.* **2006**, *5*, 219.
7. Cox, C. D.; Breslin, M. J.; Mariano, B. J. *Tetrahedron Lett.* **2004**, *45*, 1489.
8. The enantiomers were resolved by preparative HPLC with a 10 cm Chiralpak AD column using an eluant of 92% hexanes (with 0.1% diethylamine), 4% MeOH, and 4% EtOH at 150 mL/min. The first peak to elute was the inactive (*R*)-isomer and the second to elute was the (*S*)-isomer. The absolute configuration was assigned by X-ray crystallography of a ternary complex of (*S*)-7 + ADP + KSP.
9. KSP Inhibitory potency was measured with an ATPase assay. For details, see Breslin, M. J.; Coleman, P. J.; Cox, C. D.; Culberson, C. J.; Hartman, G. D.; Mariano, B. J.; Torrent, M. PCT WO 079973 A2, 2003.
10. Relative to the parental KB-3-1 cells, KB-V-1 cells, originally derived by culturing KB-3-1 cells in the presence of the Pgp substrate vinblastine (*J. Biol. Chem.* **1986**, *261*, 7762), express >500-fold higher levels of Pgp mRNA and protein. The compound potency (IC_{50}) for induction of mitotic arrest was determined by evaluating the levels of the mitotic marker phospho-nucleolin after 16 h incubation with the test compound in an 11-point half-log dilution series. The ratio of IC_{50} obtained in KB-V-1 cells versus that in KB-3-1 cells is defined as the MDR ratio. As a general guideline, we considered compounds with MDR ratios <10 to be of interest for their ability to enter and kill cells that overexpress Pgp. Verapamil, a competitive inhibitor of Pgp, restores the activity of Taxol and our KSP inhibitors in the KB-V-1 cell line to nearly that observed in the parental KB-3-1 line, confirming that Pgp efflux is responsible for the observed resistance to drug-mediated mitotic arrest.
11. Passive permeability differences may also play a role in the observed differences in the MDR ratios. Tertiary amines such as **12** have high Papp values (31.8×10^{-6} cm/s) versus primary amines such as **11** (12×10^{-6} cm/s). For a full discussion, see Ref. 5e.
12. Yan, Y.; Sardana, V.; Xu, B.; Homnick, C.; Halczenko, W.; Buser, C. A.; Schaber, M.; Hartman, G. D.; Huber, H. E.; Kuo, L. C. *J. Mol. Biol.* **2004**, *335*, 547.
13. Athymic nude mice (nu/nu) were xenografted subcutaneously with the human ovarian carcinoma cell line A2780 and the resulting tumors were allowed to reach 200–300 mm^3 before mice were surgically implanted with Alzet mini-pumps (Durect Corporation) filled with the appropriate KSP inhibitors according to manufacturer's recommendations. Prior to the implant, pumps containing KSP inhibitors were primed by incubation in 37 °C water bath for 3 h, so that the pumps would discharge KSP inhibitors at a constant rate of 8 μl/h after subcutaneous implantation. Mice were euthanized 22 h post pump implant and blood and tumors were harvested. Blood was collected in EDTA Vacutainers and processed for plasma to determine pharmacokinetics. Tumors were fixed in 10% neutral buffered formalin and then processed and embedded in paraffin. Paraffin embedded tumors were sectioned 5 μm thick and used in a phospho-Histone H3 immunohistochemistry assay designed to determine the percentage of cells blocked in mitosis compared to control treated tumors. After paraffin removal, re-hydration, and antigen retrieval, sections were incubated with anti-phospho-Histone H3 (ser10; Upstate). Following incubation with a biotinylated secondary antibody, staining of antigen positive nuclei was accomplished using avidin:biotin complexed horseradish peroxidase and diaminobenzidine reagent. Sections were imaged using an Olympus BX51 microscope with a motorized stage and Image-Pro Analysis software. Quantization of the sections was accomplished by measuring the percentage of positively stained nuclei (black) per unit area. All procedures performed on these animals were in accordance to established guidelines and were reviewed and approved by the Institutional Animal Care and Use Committee (IACUC).
14. A partial explanation for the improved in vivo activity of compound **13** versus **1** may be related to nonspecific binding in plasma. Performing the ATPase assay in the presence of human serum (+30%) increases the IC_{50} for compound **1** from 5 to 84 nM. When the same serum shift experiment is done with compound **13**, the IC_{50} increases from 2 to 20 nM.
15. Blockade of the hERG channel is associated with drug-induced prolongation of the QTc interval of the ECG, an observation that is linked to potentially fatal ventricular arrhythmias (*Torsades-de-Pointes*). The hERG IC_{50} values were determined by radioligand competition experiments using membrane preparations from HEK cells that stably express hERG. For assay details, see: Bilodeau, M. T. et al. *J. Med. Chem.* **2004**, *47*, 6363, and references therein.
16. A Herg patch clamp IC_{50} for compound **13** was determined at 7 μM. For a description of the assay, see: Wang, J.; Della Penna, K.; Wang, H.; Karczewski, J.; Connolly, T. M.; Koblan, K. S.; Bennett, P. B.; Salata, J. J. *Am. J. Physiol.* **2003**, *284*, H256.
17. Davis, F. A.; Kasu, P. V. N. *Tetrahedron Lett.* **1998**, *39*, 6135.
18. The 5*S*,2′*R* diastereomer has a KSP IC_{50} = 2.6 nM and had an EC_{50} (A2780) = 10.5 nM. Plasma half-life in the dog was 4.3 h.